RAA 2019 Vol. **19** No. **4**, 54(10pp) doi: 10.1088/1674–4527/19/4/54

http://www.raa-journal.org *http://iopscience.iop.org/raa*

***R**esearch in*
***A**stronomy and*
***A**strophysics*

Multi-aperture seeing profiler with multiple guide stars

Feng Yang[1,2,4], Gang Zhao[1,2] and De-Qing Ren[1,2,3]

[1] National Astronomical Observatories / Nanjing Institute of Astronomical Optics & Technology, Chinese Academy of Sciences, Nanjing 210042, China; *gzhao@niaot.ac.cn*

[2] CAS Key Laboratory of Astronomical Optics & Technology, Nanjing Institute of Astronomical Optics & Technology, Nanjing 210042, China

[3] Physics & Astronomy Department, California State University Northridge, 18111 Nordhoff Street, Northridge, California 91330-8268, USA

[4] University of Chinese Academy of Sciences, Beijing 100049, China

Received 2018 July 13; accepted 2018 October 24

Abstract The daytime atmospheric turbulence profile is crucial for the design of both optical systems and the control algorithm of a solar Multi-Conjugate Adaptive Optics (MCAO) system. The Multi-Aperture Seeing Profiler (MASP) is a portable instrument which can measure the daytime turbulence profile up to ~ 30 km. It consists of two portable small telescopes that can deliver performance similar to a Solar-Differential Image Motion Monitor + (S-DIMM+) on a 1.0 m solar telescope. In the original design of MASP, only two guide stars are used to retrieve the turbulence profile. In this paper, we studied the usage of multiple guide stars in MASP using numerical simulation, and found that there are three main advantages. Firstly, the precision of the turbulence profile can be increased, especially at a height of about 15 km, which is important for characterizing turbulence at the tropopause. Secondly, the equivalent diameter of MASP can be increased up to 30%, which will reduce the cost and weight of the instruments. Thirdly, the vertical resolution of the turbulence profile near the ground increases with the help of multiple guide stars.

Key words: atmospheric effects — site testing — methods: numerical

1 INTRODUCTION

The atmospheric turbulence profile, which describes the strength of turbulence at different altitudes, plays a crucial role in the design of advanced adaptive optics (AO) systems such as Ground-Layer Adaptive Optics (GLAO, Ren et al. 2015a), Multi-Conjugate Adaptive Optics (MCAO, Rimmele et al. 2010) and Tomographic Adaptive Optics (TAO, Ren et al. 2014). On one hand, a turbulence profile is important in the optical design and optimization of AO systems. In the MCAO system, deformable mirrors (DMs) are located at the conjugated heights of the turbulence layers, thus the number and conjugated heights of DMs rely on the distribution and strength of turbulence. On the other hand, the turbulence profile is also important in optimization of the control algorithm for an AO system. For example, prior information on the turbulence profile is necessary to optimize the field-of-view (FOV) of MCAO (Tokovinin et al. 2000).

Solar MCAO is crucial for solar observation, since the FOV of conventional solar AO is only about $10''$ (Beckers 1988; Rimmele & Radick 1998) and is too small for observing the solar activity region which can be as large as $1' - 2'$. In the design of solar MCAO, the daytime turbulence profile is critical. In the future, large solar telescopes, such as the Daniel K. Inouye Solar Telescope (DKIST, Elmore et al. 2014) and the European Solar Telescope (EST, Collados et al. 2010), will be equipped with MCAO systems, thus measurement of the daytime turbulence profile at these sites is important.

There are several methods to measure the turbulence profile. They are mainly divided into scintillation-based methods and slope-based methods. Scintillation-based methods such as Multi-Aperture Scintillation Sensors (MASS, Tokovinin et al. 2003) and SCIntillation Detection and Ranging (SCIDAR, Vernin & Munoz-Tunon 1994; Egner & Masciadri 2007; Avila et al. 2008) are often used

in nighttime seeing profile measurements. For daytime measurement, scintillation-based methods are only suitable to obtain the seeing profile near the ground. Beckers (2001) proposed the SHadow BAnd Ranger (SHABAR) instrument, which measured the scintillations of the whole solar disk and can only detect the seeing profile with a maximum height of $\sim$ 500 m. Slope-based methods include SLOpe Detection And Ranging (SLODAR, Wilson 2002; Butterley et al. 2006) and Solar-Differential Image Motion Monitor + (S-DIMM+, Scharmer & van Werkhoven 2010). S-DIMM+, which can detect the turbulence profile up to 30 km, is widely used in daytime turbulence profile measurements. It has been successfully applied to obtain the seeing profile with the 1.6-meter New Solar Telescope at Big Bear Solar Observatory (BBSO) (Kellerer et al. 2012) and the 1-meter Swedish Solar Telescope at La Palma (Townson et al. 2014). Using the turbulence profile of BBSO which was detected by S-DIMM+, Kellerer et al. (2012) suggested the conjugated heights of the two DMs in BBSO MCAO system to be 0 km and 3 km, and the isoplanatic angle could exceed $100''$ after AO corrections.

In S-DIMM+, the turbulence profile is measured using a wide FOV solar wavefront sensor mounted behind a solar telescope by observing the granular structure of the solar surface. Subsections on the image of each aperture serve as guide stars at different field angles. Image displacements of the subsections are used to retrieve the turbulence profile. Since this method is based on differential measurements of image displacements, it is insensitive to tracking errors and vibrations in the telescope. Based on the principle of triangulation, the sample heights of S-DIMM+ can be expressed as $h = s/\delta\alpha$, where s is the distance between any two sub-apertures and $\delta\alpha$ is angular separation between two guide stars. Therefore, the maximum measured height of S-DIMM+ is $h_{\max} = D/\delta\alpha$, where D is the diameter of the solar telescope, the vertical resolution is $\delta h = w/\delta\alpha$ and w is the size of each sub-aperture. In order to reduce cross-correlation error, the sizes of subfields are generally larger than $5''$ (Scharmer & van Werkhoven 2010; Kellerer et al. 2012; Ren et al. 2015b). Therefore a telescope with diameter of at least 0.6 m is necessary for S-DIMM+ to retrieve the turbulence profile as high as 30 km.

In order to overcome the disadvantage of S-DIMM+ which needs a large telescope, Ren et al. (2015b) introduced the idea of Multi-Aperture Seeing Profiler (MASP). The MASP consists of two small telescopes, thus it is portable and flexible for a site seeing test where no solar telescope facility can be used. A wide field Shack-Hartmann wavefront sensor (SHWFS) is equipped behind each telescope. The turbulence profile retrieval algorithm is similar to that of S-DIMM+ but with an extra term to correct the relative guide errors of the two telescopes. The equivalent diameter of MASP is about three times that of small telescopes. Using two small telescopes with diameter of 400 mm, MASP can achieve similar performance as an S-DIMM+ with a 1120 mm telescope and is able to retrieve the turbulence profile up to 30 km.

In S-DIMM+ measurement, multiple guide stars can be used to increase the precision of turbulence retrieval since more independent measurements can be done. Furthermore, fewer sub-apertures are needed to measure the turbulence profile with multiple guide stars. Waldmann et al. (2007); Waldmann et al. (2008) proposed a method similar to S-DIMM+, but with fewer sub-apertures and many more field directions. Ren & Zhao (2016) introduced the idea of an Advanced Multi-Aperture Seeing Profiler (A-MASP). In A-MASP, only two smaller telescopes (or two sub-apertures) with no SHWFS are used to measure the turbulence profile up to 20 km. Using the idea of A-MASP, the turbulence profile above the site of the Dunn Solar Telescope (DST) at National Solar Observatory is measured by Ren et al. (2018). Multiple guide stars can also help to increase the vertical resolution of the turbulence profile. In Scharmer & van Werkhoven (2010), multiple guide stars are applied to increase the resolution of the turbulence profile near the ground. Wang et al. (2018) showed that additional height grids for characterizing daytime seeing profiles can be introduced if multiple guide stars are utilized.

In this publication, implementing multiple guide stars in MASP will be studied. If multiple guide stars are used, the precision of the turbulence profile as well as the configuration of MASP can both be improved. This paper is organized as follows. In Section 2, the turbulence retrieval algorithm of MASP is described. In Section 3, we compare the precision of MASP with two guide stars and multiple guide stars using numerical simulation. In Section 4, we show that the configuration of MASP can be improved with the help of multiple guide stars. In Section 5, the issue of vertical resolution of the turbulence profile is discussed. A summary is provided in Section 6.

2 TURBULENCE PROFILE RETRIEVAL ALGORITHM OF MASP

An MASP consists of two portable small telescopes instead of a single large aperture. Behind each telescope, a wide-field SHWFS is mounted. Figure 1 shows the layout of the MASP. The two circles indicate the apertures of

the small telescopes and the grid shows the sub-apertures of the SHWFS with size of $w \times w$. The lenslet array of the SHWFS is along the line connecting the centers of the two apertures, which is set to be the x-direction. A gap exists between the two small telescopes and is indicted by grids of dotted lines. We mainly use the center row of the sub-apertures to retrieve the turbulence profile, and they are numbered in the figure.

In the measurement, the same region of solar surface is observed simultaneously by the two telescopes. Subfields with a size of $\theta \times \theta$ are selected from the image of each sub-aperture, and they serve as guide stars. (Hereafter we will call these subfields guide stars for simplicity.) The guide stars are uniformly distributed along the x-direction, with $\Delta\alpha$ between two adjacent guide stars. For the i-th guide star, its field angle is represented as α_i.

Using image cross-correlation, the x-component of the displacement of the i-th guide star in two sub-apertures can be measured as $\delta x(s, \alpha_i)$, where s is the distance between the two sub-apertures. For the case that the two sub-apertures are located on different telescopes, we have $\delta x(s, \alpha_i) = \delta\tilde{x}(s, \alpha_i) + \delta x_{\rm tel}$, where $\delta\tilde{x}(s, \alpha_i)$ is the displacement made from atmospheric turbulence and $\delta_{\rm tel}$ is the displacement caused by errors in the direction of the telescopes. When the two sub-apertures are in the same telescope, $\delta x(s, \alpha_i) = \delta\tilde{x}(s, \alpha_i)$.

When the two sub-apertures are in the same telescope, we can directly use the turbulence profile retrieval algorithm of S-DIMM+ (Scharmer & van Werkhoven 2010). Assuming that the guide star displacement is due to added contributions from N turbulence layers located at heights h_n, the covariance between two guide stars can be expressed as

$$\langle \delta x(s, \alpha_i), \delta x(s, \alpha_j) \rangle = \sum_{n=1}^{N} c_n F_x \left(s, \alpha_i - \alpha_j, h_n\right), \quad (1)$$

and

$$\langle \delta y(s, \alpha_i), \delta y(s, \alpha_j) \rangle = \sum_{n=1}^{N} c_n F_y \left(s, \alpha_i - \alpha_j, h_n\right) , \quad (2)$$

where c_n indicates the strength of the turbulence layers, and F_x, F_y have the following expressions

$$\begin{aligned} F_x(s, \alpha, h) =& I[(\theta h - s)/D_{\rm eff}, 0]/2 \\ &+ I[(\theta h + s)/D_{\rm eff}, 0]/2 \\ &- I[\theta h/D_{\rm eff}, 0], \\ F_y(s, \theta, h) =& I[(\theta h - s)/D_{\rm eff}, \pi/2]/2 \\ &+ I[(\theta h + s)/D_{\rm eff}, \pi/2]/2 \\ &- I[\theta h/D_{\rm eff}, \pi/2]. \end{aligned} \quad (3)$$

$I(u, 0)$ and $I(u, \pi/2)$ are the atmospheric structure functions and $D_{\rm eff} = w + \theta h_n$ is the effective diameter. For the circular apertures we used, $I(u, 0)$ and $I(u, \pi/2)$ have the forms according to Kellerer (2015)

$$\begin{aligned} I(u, 0) &= 2 - |1 - u|^{5/3} + 2|u|^{5/3} - |1 + u|^{5/3}, \\ I(u, \pi/2) &= 2 + 2|u|^{5/3} - 2(1 + u^2)^{5/6}. \end{aligned} \quad (4)$$

When the two sub-apertures are located in different telescopes, we follow the turbulence profile retrieval algorithm of MASP (Ren et al. 2015b). For individual exposures, the orientations of the telescopes are fixed and $\delta x_{\rm tel}$ is also a fixed value for each guide star. Thus the differential value of $\delta x(s, \alpha_i)$ and $\delta x(s, \alpha_j)$ will no longer contain the orientation error

$$\langle [\delta x(s, \alpha_i) - \delta x(s, \alpha_j)]^2 \rangle = \langle [\delta\tilde{x}(s, \alpha_i) - \delta\tilde{x}(s, \alpha_j)]^2 \rangle \ . \quad (5)$$

Expanding it, we can have

$$\langle \delta x(s, \alpha_i), \delta x(s, \alpha_j) \rangle = \sum_{n=1}^{N} c_n F_x \left(s, \alpha_i - \alpha_j, h_n\right) + \Delta_x \ , \quad (6)$$

where

$$\Delta_x = \langle \delta x^2(\alpha_i) \rangle/2 + \langle \delta x^2(\alpha_j) \rangle/2 - \sum c_n I(s/D_{\rm eff}, 0) \ . \quad (7)$$

Similarly for y-direction, we have

$$\langle \delta y(s, \alpha_i), \delta y(s, \alpha_j) \rangle = \sum_{n=1}^{N} c_n F_y \left(s, \alpha_i - \alpha_j, h_n\right) + \Delta_y \ , \quad (8)$$

where

$$\Delta_y = \langle \delta y^2(\alpha_i) \rangle/2 + \langle \delta y^2(\alpha_j) \rangle/2 - \sum c_n I(s/D_{\rm eff}, \pi/2) \ . \quad (9)$$

Then the array of equations can be listed using Equations (6) and (8), and c_n can be solved, which is related to the Fried parameter r_0 of the layer at h_n through

$$c_n = 0.358 \lambda^2 r_0^{-5/3}(h_n) D_{\rm eff}^{-1/3}(h_n) \ , \quad (10)$$

where λ is the wavelength and z is the zenith angle. We can also express the results in terms of the atmospheric refractive index of each layer as

$$C_n^2(h_n) = 0.16 D_{\rm eff}^{-1/3}(h_n) \cos(z) c_n \ . \quad (11)$$

3 PRECISION OF MASP WITH MULTIPLE GUIDE STARS

In the original design of MASP, only two guide stars were used. If we increase the number of guide stars, for each s and $\delta\alpha$, more independent measurements can be done. For

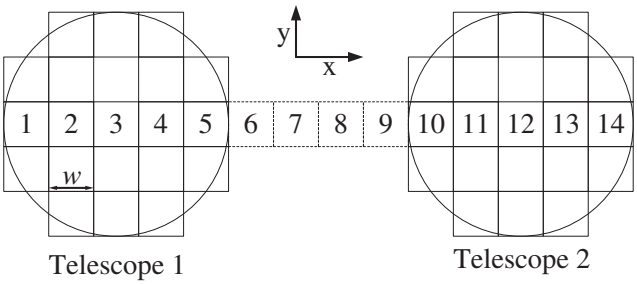

Fig. 1 Layout of the MASP. Two *circles* indicate the two small telescopes. Grids in *solid lines* show the layout of the SHWFS, and the grid of *dashed lines* indicates the gap between the two telescopes.

example, if four guide stars are implemented, we will have as many as six times more independent measurements than those in the case of two guide stars, which could increase the precision of the turbulence profile measurement. In this section, we will use numerical simulation to study the precision of MASP with multiple guide stars in detail.

3.1 Numerical Method

We employ a Monte Carlo numerical simulation to study the seeing retrieval process, which is similar as those in Ren et al. (2015b) and Ren & Zhao (2016). Here are details about the simulations.

(1) Kolmogorov phase screens are obtained for each layer according to Johansson & Gavel (1994).
(2) The sub-section of a phase screen projected to the pupil plane for each guide star and each sub-aperture is selected.
(3) The shift values of the guide stars are calculated according to the slope of the phase screen. Note that we use the shift value of a guide star at the center of the subfield to represent the shifts of the whole small range of the image. In our study, we focus on how multiple guide stars will affect the results, thus using guide stars instead of extended targets will make the simulation faster and simpler. The difference between extended target and guide star has been studied in Ren & Zhao (2016), which demonstrates that this approach to the simulation is reasonable in this study.
(4) Guide errors of the telescope are considered. For each simulated exposure frame, two random numbers are generated to simulate the orientation errors of the two telescopes, and then they are added to the shift values of guide stars observed by the first and second telescopes, respectively. We arbitrarily assume the orientation errors of the two telescopes are both $10''$. In the turbulence retrieval process, the orientation errors can be totally eliminated in Equations (6) and (8).
(5) The covariances of the shift between guide stars are calculated. For each s and $\delta\alpha$, there could be more than one group of independent measurements. For example, the shift values from sub-apertures 1 and 3 and guide stars α_1 and α_3, and sub-aperture 2 and 4 and guide stars α_2 and α_4 will both have $C(2w, 2\Delta\alpha)$, where w is the distance between two adjacent sub-apertures, and $\Delta\alpha$ is the angular separation between the adjacent guide stars. For each $s, \delta\alpha$ combination, all the independent measurements are averaged to be $C_x(s, \delta\alpha)$ and $C_y(s, \delta\alpha)$ for the x and y directions respectively, and the number of independent measurements is expressed by $W(s, \delta\alpha)$.
(6) N layers in the grid of sample heights h_n are decided. Then an array of linear equations can be built. To obtain the unknown coefficients c_n in Equations (6) and (8), we can solve a conventional linear least-squares fit problem by minimizing the badness parameter L, given by

$$L = \sum_{s,\delta\alpha} \left(\left[C_x(s,\delta\alpha) - \sum_n c_n F_x(s,\delta\alpha,h_n) - \Delta_x \right]^2 + \left[C_y(s,\delta\alpha) - \sum_n c_n F_y(s,\delta\alpha,h_n) - \Delta_y \right]^2 \right) \times W^2(s,\delta\alpha). \tag{12}$$

Since c_n cannot be negative, we use the $nnls$ function in the *scipy.optimize* package to solve this equation. After c_n is found, we will use Equations (10) and (11) to calculate $r_0(h_n)$ and $C_n^2(h_n)\mathrm{d}h$.

3.2 Initial Setup

The layout of the MASP we studied is shown in Figure 1. Two small telescopes with apertures of 400 mm are used to form the MASP. An SHWFS is located behind each telescope. The size of a sub-aperture $w = 80$ mm and there are five sub-apertures crossing the diameter of each telescope.

The edge-to-edge distance of the two telescopes is $4w$ (about 320 mm). Due to the configuration, the maximum distance between two sub-apertures in one telescope is $4w$, while the minimum distance between two sub-apertures in different telescopes is $5w$, thus s can be continuously increased from $1w$ to $13w$, which is the same as in an S-DIMM+ instrument on a 1120 mm telescope. Six guide stars along the x-direction (line connecting the center of the telescopes) are simulated, and the angular separation between the adjacent guide stars is $\Delta\alpha = 5.5''$.

3.3 One-layer Case

In order to test the precision of the retrieved turbulence, we start with a simple case in which only one layer of turbulence is considered. In this simulation, the turbulence layer is located from 0 km to 30 km with $r_0 = 0.1$ m. Four-thousand frames of data are simulated and are divided into eight bursts. In the seeing retrieval process, we assume that the height of the turbulence layer is already known. For each burst of data, r_0 is retrieved using 500 frames of data.

In Figure 2(a) and (b), the values and relative errors of r_0 are plotted, respectively. The black solid line represents the input r_0 with value of 0.1 m. The blue dotted line, orange dashed line and green dot-dashed line indicate the results of 2, 4, and 6 guide stars cases, respectively. It can be seen from the figure that the turbulence layers at different heights can be retrieved well for all of the three cases with $< 10\%$ difference from the input values. We estimate the error of r_0 using the standard deviation of r_0 for eight bursts of data, and they are plotted in Figure 2(b). For the layers lower than 6 km, r_0 can be retrieved accurately for all of the three cases, with maximum error $< 4\%$ (2 star case) and $< 2.5\%$ (4 or 6 star cases). After 9 km, the errors increase with height and have peaks at around 12 – 18 km. The maximum relative errors of the three cases are 6.8%, 5.5% and 3.2% respectively. After 18 km, the errors decrease to low values again for all three cases. Generally, we can see that the errors in r_0 decrease with the increase in the number of guide stars, except for some particular heights. (For example at 12 km, error of the 4 guide star case is greater than that of the 2 guide star case).

MASP is based on the principle of trigonometry that can be applied to measure the turbulence profile. For the case that the distance between two sub-apertures is s and the angular separation between two guide stars is $\delta\alpha$, the corresponding measured height is $s/\delta\alpha$. For a certain height at $s/\delta\alpha$, there may be several independent measurements of it. Firstly, we can choose different start sub-apertures (or reference sub-apertures). For example, sub-aperture pairs (1, 3), (2, 4) and (3, 5) all have a distance of $2w$. Secondly, the start guide stars can also be changed if multiple guide stars are used. For example, for $\delta\alpha = 2\Delta\alpha$, we can use guide star pairs (α_1, α_3) or (α_2, α_4). Thirdly, s and $\delta\alpha$ can be both changed at the same time. For example, the turbulence layer at $w/\Delta\alpha$ corresponds to both $(w, \Delta\alpha)$ and $(2w, 2\Delta\alpha)$.

In Figure 3, we plot the numbers of independent measurements for each corresponding height. In panel (a), the results of the two-guide star case are plotted. Since only two guide stars are used, the number of measurements is mainly due to the change in start sub-aperture. Because sub-apertures 6 – 9 are missing in MASP, the number of measurements decreases to one at 15 km. For the r_0 retrieval results in Section 3.3, r_0 has the largest error around 18 km, which is due to the decreased number of measurements there. If 4 or 6 guide stars are used (panel (b) and panel (c) respectively), we can see that the number of measurements for each layer increases, which can lead to an increase in the precision. From the figure, we can also see that the sample heights are much denser with multiple guide stars, especially near the ground layer. This feature can be used to increase vertical resolution of the turbulence profile, which will be discussed in Section 5.

3.4 Multi-layer Case

In the above simulations, we assume that the layer heights are known in advance to study the precision of the turbulence profile. However, the heights of the turbulence layers in fact also need to be retrieved. In this sub-section, we will use multiple layers to sample the input turbulence profile. The input turbulence profile is arbitrary with turbulence layers at 0 km, 6 km, 12 km, 18 km, 24 km and 30 km, and the total r_0 is 0.1 m. We use 11 layers located from 0 to 30 km with a 3 km separation to sample the turbulence profile. Namely, $N = 11$ and $h_n = n \times 3$ km in Equations (6) and (8). In the simulation, 4000 frames are generated and used to retrieve the profile.

In Figure 4, we plot the results. In the figure, the black solid line is the input C_N^2, and the blue dotted line, orange dashed line and green dot-dashed line represent the 2, 4 and 6 guide star cases, respectively. For the 2 guide star case, we can see that the layer at 12 km cannot be measured well. This is consistent with the results of Section 3.3 in which only one layer is considered and the layers between 12 km and 18 km have large retrieval errors. We can also see that the 4 guide star and 6 guide star cases have similar performances and both provide a precise turbulence profile.

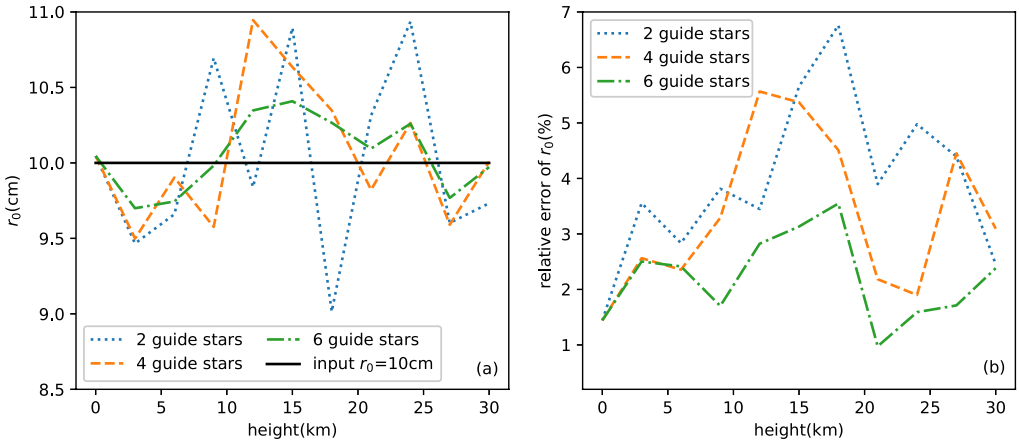

Fig. 2 One-layer case: the results of retrieved r_0 with different numbers of guide stars. (a) the values of retrieved r_0 with 500 frames of data; the input r_0 is 0.1 m. (b) relative errors of r_0 with eight bursts of 500 frames of data.

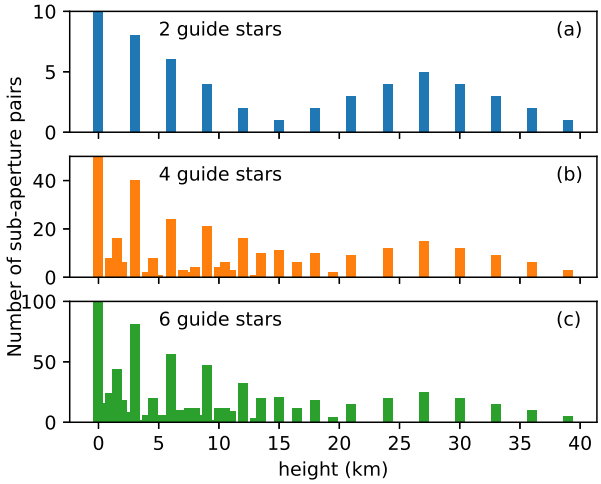

Fig. 3 The counts of independent measurement versus the corresponding sample height.

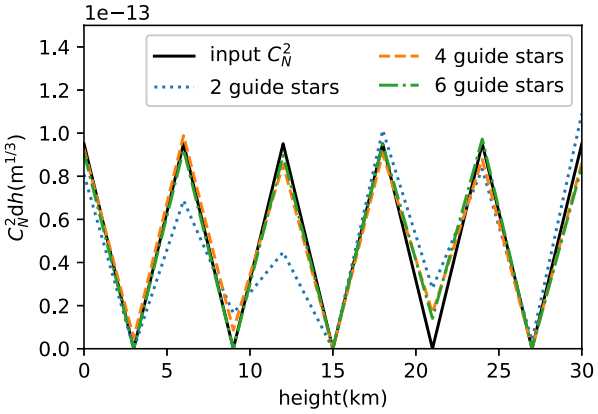

Fig. 4 Multi-layer case: the simulation result of retrieved $C_N^2 \mathrm{d}h$, turbulence profile located at six layers, from 0 km to 30 km, with an interval of 6 km for each layer.

According to the atmospheric theories, high-altitude turbulence is located at the tropopause with an altitude of about 9 – 18 km. However at these heights, the MASP instruments have large detection errors if only two guide stars are used, since the sub-apertures corresponding to those heights are missing due to using two small telescopes. In this section, we found that if multiple guide stars are used, this disadvantage of MASP will be overcome and the turbulence layer at different heights can be measured with high precision.

4 INCREASING THE SEPARATION OF THE TWO TELESCOPES THAT ARE PART OF MASP

In the original design of MASP with two guide stars, the separation between the two small telescopes is restricted to be smaller than the diameter of the small telescopes. Otherwise, the turbulence layer around a certain height cannot be detected. If multiple guide stars are used, fewer sub-apertures or larger separation between telescopes is possible. In this section, we will test the turbulence profile retrieval process using another configuration of MASP with small telescopes and large separation, which is shown in Figure 5. The size of each telescope is 320 mm, which is equal to $4w$ (four sub-apertures are crossing the aperture). The separation between the two telescopes is set to 480 mm ($6w$). The equivalent size of the new configuration is still 1120 mm, the same as the original one.

In Figure 6, the number of independent measurements versus the corresponding sample heights is plotted, which is similar to Figure 3. In the new configuration, the maximum separation of sub-apertures in a single telescope is $3w$, and the minimum separation of sub-apertures in different telescopes is $7w$. Therefore there is no sub-aperture pair with distances of $4w$, $5w$ or $6w$, and the corresponding turbulence layers from 12 km to 18 km cannot be measured (see panel (a) of Fig. 6). While multiple guide stars are used, the turbulence at 12 km, 15 km and 18 km can be measured using the combination of $(8w, 2\Delta\alpha)$, $(10w, 2\Delta\alpha)$ and $(12w, 2\Delta\alpha)$, respectively. Thus we infer that MASP with smaller telescopes will have similar performance.

We repeat the numerical simulation in Section 3 to test the performance of MASP with smaller telescopes. In Figure 7, the results of the one-layer case are plotted. From Figure 7(a), we can see if only 2 guide stars are used, r_0 of the layers at about 15 km will have extremely large errors and cannot be measured. For the 4 guide star and 6 guide star cases, the new configuration of MASP works well, and each layer can be retrieved with error $< 7\%$. For both the 4 star case and 6 star cases, the standard error curves also have a peak at about 15 km with value of 6.9% and 5.1%. Compared with the results of the standard MASP, which has maximum errors of 5.5% and 3.2% for 4 and 6 guide stars respectively, the precision of the new configuration is slightly lower but acceptable.

In Figure 8, we plot the simulation results in which multiple turbulence layers are considered. The initial setup is the same as that in Section 3.4. Six layers of input turbulence profile are considered in the simulation, which are located from 0 km to 30 km, with separation of 6 km between two adjacent layers. For the 2 guide star case (blue dotted line), the turbulence layer at 12 km and 18 km cannot be measured. The turbulence layer of these two layers contributes to the lower layers, which leads to overestimating the strength of the lower layers. When we use 4 guide stars (orange dashed line), the C_N^2 can be retrieved well. When 6 guide stars are used (green dot-dashed line), we will have a more accurate result, similar to the results of standard MASP.

In the new configuration of MASP, two telescopes with diameter of 320 mm are used, and it has similar performance to the original design of MASP with 400 mm telescopes as well as an S-DIMM+ instrument on a 1 m telescope with 14 apertures crossing the diameter.

For the general case of MASP, we assume that the two telescopes have N apertures crossing their diameters, and the separation of the two telescopes is equal to M times the size of a sub-aperture. Using these assumptions, the distances between sub-aperture pairs in one telescope are from 1 to $N-1$, while the distances between sub-aperture pairs in different telescopes are from $M+1$ to $2N+M-1$. If $N-1 \geq (M+1)-1$ (namely $M \leq N-1$), the distances of sub-aperture pairs can be continuously increased from 1 to $M+N$, and two guide stars are enough to sample the turbulence profile. When two guide stars are used, the maximum equivalent diameter of the MASP is $w(M+2N) = (3N-1)w$, which is about three times the diameter of each telescope. If multiple guide stars are used, we can have additional sample heights using guide stars with larger angular separation. For example, if the two guide stars have separations of $2\Delta\alpha$, additional sample heights from $w(M+1)/(2\Delta\alpha)$ to $w(2N+M+1)/(2\Delta\alpha)$ can be applied in the turbulence retrieval. These additional sampled heights would only cover the gap in sub-aperture distance if $(2N+M-1)/2 \geq (M+1)-1$ and $(M+1)/2-1 \leq (N-1)$. These two inequalities are equivalent to $M \leq 2N-1$, which means the maximum equivalent diameter of the MASP with multiple guide stars is $w(M+2N) = (4N-1)w$, four times the diameter of the

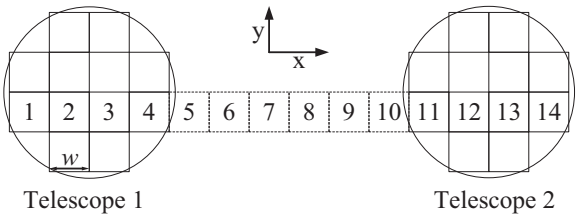

Fig. 5 Similar to Fig. 1, but with smaller telescopes and a bigger gap between the two telescopes.

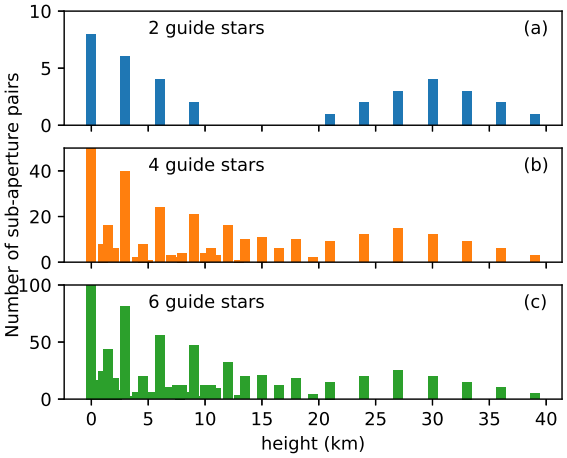

Fig. 6 Similar to Fig. 3, but demonstrating that the turbulence layers at 12 km to 18 km cannot be measured for the 2 guide star case.

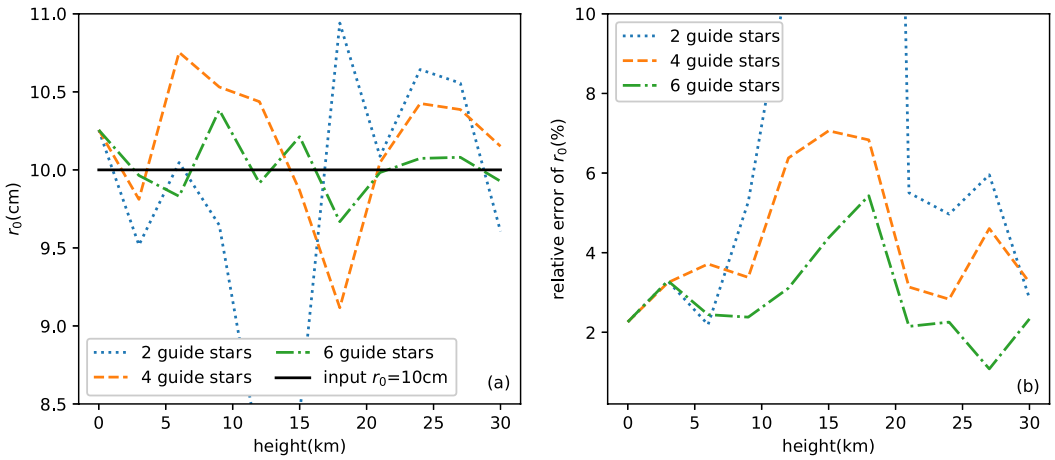

Fig. 7 Similar to Fig. 2, but when two guide stars are used, at some heights like 12 km, r_0 cannot be measured.

small telescope. Thus the equivalent diameter of the MASP will be increased by $(4N-1-3N+1)/(3N+1) \approx 30\%$.

5 DISCUSSION

The vertical resolution of S-DIMM+ can be increased if multiple guide stars are used, which have been well studied by Wang et al. (2018). For the MASP, the vertical resolution can also be increased. In Figure 3 and Figure 6, we can see that the distance between heights is much denser if 4 or 6 guide stars are used. In our previous simulations of multi-layer cases, the height grid is uniform with vertical resolution of 3 km, and the vertical resolution can be increased if we use a nonuniform sample grid.

In Figure 9(a), we plot the cumulated $C_N^2 dh$ using different guide stars. The meaning of each curve is the same as those in Figures 4 and 8 and the solid points indicate the

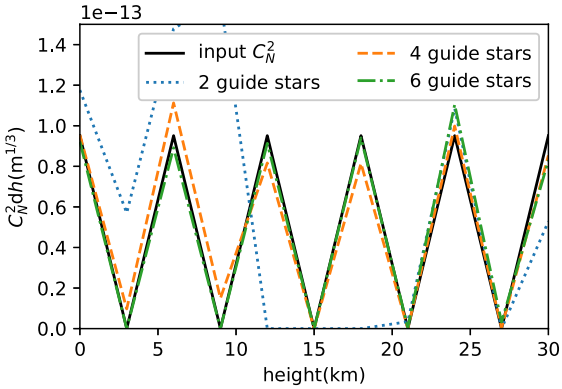

Fig. 8 Similar to Fig. 4, but demonstrating that the turbulence layer at 12 km and 18 km cannot be measured for the 2 guide star case.

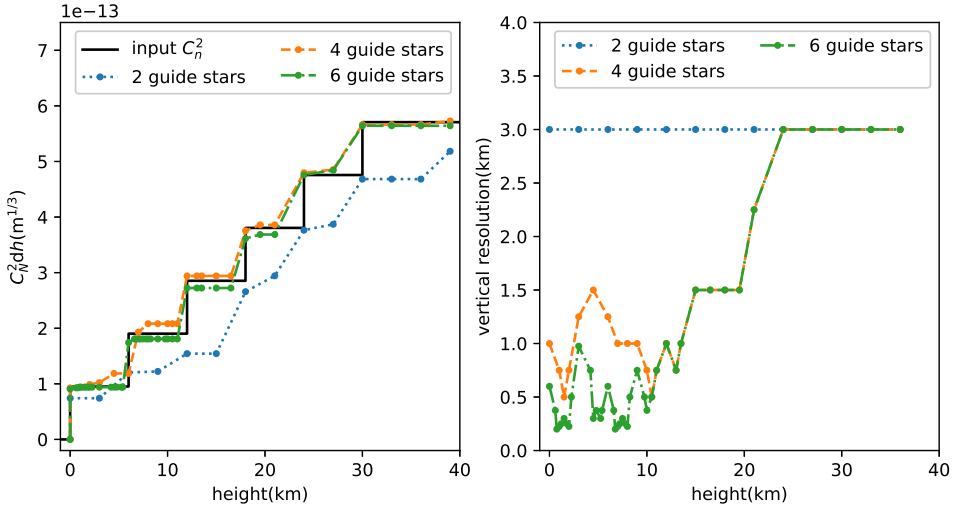

Fig. 9 Increasing the vertical resolution by using multiple guide stars. (a) The cumulated $C_N^2 dh$ using different guide stars. (b) The vertical resolution at different heights.

height grid. It can be seen that with multiple guide stars, the vertical resolution can be dramatically increased near the ground. The vertical resolution at different heights is estimated in Figure 9(b). If two guide stars are used, the vertical resolutions are 3 km for all the layers. When multiple guide stars are used, the vertical resolution for the turbulence layer below 10 km is about 0.5 km to 1 km. If 6 guide stars are used, the vertical resolution can be as high as 0.2 km. In the daytime, cool nocturnal air warms up, thus turbulence near the ground becomes stronger. Using multiple guide stars, we can characterize the strong daytime ground turbulence layer better.

6 CONCLUSIONS

The daytime turbulence profile is important for the design of both optics and the control algorithm of a solar MCAO. Currently, S-DIMM+ is the most useful method to measure the daytime turbulence profile up to 30 km. However, S-DIMM+ needs to use a solar telescope with a diameter of about 1 m, which limits the use of S-DIMM+ in a site survey. The MASP consists of two small telescopes and is portable for site seeing tests. Using the turbulence profile retrieval algorithm similar to S-DIMM+, MASP can measure the turbulence profile up to 30 km. In the original design of MASP, only two guide stars are used. In this paper, we aim to use multiple guide stars to improve the performance of MASP.

We find that when using multiple guide stars, the precision of the turbulence profile by MASP can be increased, especially for turbulence layers at 12 – 18 km where high altitude turbulence layers at the tropopause are mainly located. Thus using multiple guide stars, MASP can provide better measurement of high-altitude turbulence.

A new configuration of MASP was introduced which consists of two 320 mm telescopes. If multiple guide stars are used, it will have the same equivalent diameter as the original design of MASP with 400 mm telescopes. This means using multiple guide stars, with which the equivalent diameter of MASP can be increased up to 30%.

The vertical resolution of MASP is also studied. If multiple guide stars are used, vertical resolution near the ground can be increased from 3 km to ~ 0.5 km in the case that we studied. Thus, strong ground turbulence in the daytime can be better characterized.

Acknowledgements This work was supported by the National Natural Science Foundation of China (Nos. 11873068, 11433007, 11661161011 and 11673042), the Strategic Priority Research Program of the Chinese Academy of Sciences (XDA15010300), the International Partnership Program of Chinese Academy of Sciences (114A32KYSB20160018 and 114A32KYSB20160057), the special funding for Young Researchers at Nanjing Institute of Astronomical Optics & Technology and part of this work was carried out at CSUN, with support from NSF (Grant AST-1607921).

References

Avila, R., Avilés, J. L., Wilson, R. W., et al. 2008, MNRAS, 387, 1511

Beckers, J. M. 1988, in Very Large Telescopes and Their Instrumentation, 2, 693

Beckers, J. M. 2001, Experimental Astronomy, 12, 1

Butterley, T., Wilson, R. W., & Sarazin, M. 2006, MNRAS, 369, 835

Collados, M., Bettonvil, F., Cavaller, L., et al. 2010, in Proc. SPIE, 7733, Ground-based and Airborne Telescopes III, 77330H

Egner, S. E., & Masciadri, E. 2007, PASP, 119, 1441

Elmore, D. F., Rimmele, T., Casini, R., et al. 2014, in Proc. SPIE, 9147, Ground-based and Airborne Instrumentation for Astronomy V, 914707

Johansson, E. M., & Gavel, D. T. 1994, in Proc. SPIE, 2200, Amplitude and Intensity Spatial Interferometry II, ed. J. B. Breckinridge, 372

Kellerer, A. 2015, arXiv:1504.00320

Kellerer, A., Gorceix, N., Marino, J., Cao, W., & Goode, P. R. 2012, A&A, 542, A2

Ren, D., Zhu, Y., Zhang, X., Dou, J., & Zhao, G. 2014, Appl. Opt., 53, 1683

Ren, D., Jolissaint, L., Zhang, X., et al. 2015a, PASP, 127, 469

Ren, D., Zhao, G., Zhang, X., et al. 2015b, PASP, 127, 870

Ren, D., & Zhao, G. 2016, PASP, 128, 105002

Ren, D., Zhao, G., Wang, X., et al. 2018, Solar Physics, in press

Rimmele, T. R., & Radick, R. R. 1998, in Proc. SPIE, 3353, Adaptive Optical System Technologies, eds. D. Bonaccini, & R. K. Tyson, 72

Rimmele, T. R., Woeger, F., Marino, J., et al. 2010, in Proc. SPIE, 7736, Adaptive Optics Systems II, 773631

Scharmer, G. B., & van Werkhoven, T. I. M. 2010, A&A, 513, A25

Tokovinin, A., Kornilov, V., Shatsky, N., & Voziakova, O. 2003, MNRAS, 343, 891

Tokovinin, A., Le Louarn, M., & Sarazin, M. 2000, Journal of the Optical Society of America A, 17, 1819

Townson, M. J., Kellerer, A., Osborn, J., et al. 2014, in Proc. SPIE, 9147, Ground-based and Airborne Instrumentation for Astronomy V, 91473E

Vernin, J., & Munoz-Tunon, C. 1994, A&A, 284, 311

Waldmann, T. A., Berkefeld, T., & von der Lühe, O. 2007, in Adaptive Optics: Methods, Analysis and Applications, Optical Society of America, PMA3

Waldmann, T. A., Berkefeld, T., & von der Lühe, II, O. 2008, in Proc. SPIE, 7015, Adaptive Optics Systems, 70155O

Wang, Z., Zhang, L., Kong, L., et al. 2018, MNRAS, 478, 1459

Wilson, R. W. 2002, MNRAS, 337, 103